European Review for Medical and Pharmacological Sciences 2023; 27: 5692-5699

A decision tree model to distinguish between benign and malignant pulmonary nodules on CT scans

X.-B. MA[1], Q.-L. XU[2], N. LI[3], L.-N. WANG[4], H.-C. LI[2], S.-J. JIANG[1]

[1]Department of Respiratory Medicine, Shandong Provincial Hospital, Shandong University, Jinan, China
[2]Department of Respiratory Medicine, Provincial Hospital Affiliated to Shandong First Medical University, Jinan, China
[3]Department of Radiology, Provincial Hospital Affiliated to Shandong First Medical University, Jinan, China
[4]Department of Medical Imaging, Provincial Hospital Affiliated to Shandong First Medical University, Jinan, China

Quanlin Xu and Xiaobin Ma contributed equally to this work

Abstract. – OBJECTIVE: Chest computed tomography (CT) is increasingly being used to screen for lung cancer. Machine learning models could facilitate the distinction between benign and malignant pulmonary nodules. This study aimed to develop and validate a simple clinical prediction model to distinguish between benign and malignant lung nodules.

PATIENTS AND METHODS: Patients who underwent a video thoracic-assisted lobectomy between January 2013 and December 2020 at a Chinese hospital were enrolled in the study. The clinical characteristics of the patients were extracted from their medical records. Univariate and multivariate analyses were used to identify the risk factors for malignancy. A decision tree model with 10-fold cross-validation was constructed to predict the malignancy of the nodules. The sensitivity, specificity, and area under the curve (AUC) of a receiver operatic characteristics curve were used to evaluate the model's prediction accuracy in relation to the pathological gold standard.

RESULTS: Out of the 1,199 patients with pulmonary nodules enrolled in the study, 890 were pathologically confirmed to have malignant lesions. The multivariate analysis identified satellite lesions as an independent predictor for benign pulmonary nodules. Conversely, the lobulated sign, burr sign, density, vascular convergence sign, and pleural indentation sign were identified as independent predictors for malignant pulmonary nodules. The decision tree analysis identified the density of the lesion, the burr sign, the vascular convergence sign, and the drinking history as predictors of malignancy. The area under the curve of the decision tree model was 0.746 (95% CI 0.705-0.778), while the sensitivity and specificity were 0.762 and 0.799, respectively.

CONCLUSIONS: The decision tree model accurately characterized the pulmonary nodule and could be used to guide clinical decision-making.

Key Words:
Decision tree model, Pulmonary nodules, Malignant, Benign.

Introduction

Lung cancer is the leading cause of cancer-related deaths worldwide. Smoking and pollution can increase the risk of developing lung cancer[1]. Non-small cell lung cancer (NSCLC) accounts for approximately 85% of lung cancer diagnoses. However, due to the lack of early diagnostic tools, approximately 50% of NSCLC patients are found at stage IV, and their 5-year survival rate is lower than 10%[2]. High-resolution computed tomography (CT) and low-dose computed tomography (LDCT) are increasingly being used to screen for lung cancer[3,4]. These imaging techniques can detect very small pulmonary nodules. However, not all of these nodules are found to be malignant after biopsy. Several features could be used to discriminate between benign and malignant lesions, including lesion size, the proportion of solid components, and density[5]. According to the above malignant characteristics, more and more surgical interventions for pulmonary nodules are being performed. With the advancement of medical

Corresponding Authors: Huaichen Li, MD; e-mail: lihuaichen@163.com; Shujuan Jiang, MD; e-mail: docjiangshujuan@163.com

technology, video-assisted thoracoscopic surgery (VATS) for lobectomy is becoming the mainstream surgical method[6]. However, the distinction between benign and malignant pulmonary nodules based on these features remains very subjective and prone to errors. As a result, patients may end up undergoing invasive biopsies, leading to increased healthcare costs and unnecessary anxiety. Therefore, new techniques are needed to facilitate the distinction between benign and malignant pulmonary nodules identified on CT.

Radiomics uses advanced computational and statistical methods to extract a large number of features from medical images to detect disease and predict treatment outcomes. This technique is increasingly being used to characterize pulmonary nodules[7,8]. Nevertheless, the use of radiomics to distinguish between benign and malignant nodules remains controversial. The implementation of artificial intelligence (AI) technology based on deep learning in radiology is improving diagnostic accuracy, feature detection, and patient follow-up. However, this system is expensive, and a number of primary hospitals are unable to be equipped with it. Simpler models based on clinical and imaging features could be used to facilitate the characterization of pulmonary lesions.

As a result, in this study, we aimed to develop a simple decision tree model to characterize pulmonary nodules identified on CT.

Patients and Methods

Study Population

All patients who underwent a video-assisted thoracoscopic surgery (VATS) lobectomy from January 2013 to December 2020 at the Provincial Hospital Affiliated with Shandong First Medical University were eligible for the study. All patients had conclusive postoperative pathological results. Patients with pulmonary nodules with a diameter greater than 2 cm and unclear borders were excluded. In addition, patients with extrapulmonary tumors or multiple mediastinal lesions confirmed by auxiliary examinations were also excluded.

Ethical Considerations

The study was conducted according to the guidelines of the Declaration of Helsinki and approved by the Ethics Committee of The Provincial Hospital Affiliated with Shandong First Medical University.

Patient Characteristics

The clinical characteristics, including; gender, age, occupation, smoking history, drinking history, and family history, were extracted from the patient's medical records.

Image Acquisition and Analysis

Two trained radiologists independently interpreted the chest CT of each patient. The radiologists were blinded to the pathological results. They were asked to record the nodule features, including location, diameters, lobulation, burr, boundary, satellite lesions, density (solid, subsolid, ground glass), vacuoles/calcifications, vascular bundle sign, pleural depression sign, mediastinal lymph nodes. They also classified solitary pulmonary nodules into solid (SN) and subsolid nodules (SSN). The SSNs were further classified into ground glass nodules (GGNs) and subsolid nodules[9]. In addition, the GNSs were divided into indeterminate, high-density opacities showing bronchial vascular structures[10].

Statistical Analysis

The Chi-squared (χ^2) test was used to compare the categorical data, while the Student's *t*-test was used to compare the continuous data between the malignant and benign nodules. Odds ratios (ORs) with 95% confidence intervals (CIs) were used to estimate the effective size and variability. Univariate analysis was performed to identify the clinical and imaging features that differed significantly between the benign and malignant groups. The significantly different features were then included in the multivariate logistic regression analysis to identify the independent risk factors for malignancy. A forest plot was used to illustrate the results of the multivariate analysis. The independent risk factors were then used to build a decision tree model to categorize the patients into high, medium, and low-risk groups based on clinical and imaging features[11]. Ten-fold cross-validation was used to minimize the risk of overfitting the model.

The area under the curve (AUC) of a receiver operating characteristic (ROC) curve was used to assess the discriminative power of the decision tree model. The one-way analysis of variance (ANOVA) and Tamhane's T2 posthoc analysis were used to analyze the AUC. For this analysis, the significance level α was set at 0.001. All statistical analyses were performed using the R software (available at: https://www.r-project.org), version 3.4.3, and a two-sided *p*-value below 0.05 was considered statistically significant.

Results

Clinical and Nodule Characteristics

A total of 1,199 patients with pulmonary nodules who underwent a VATS lobectomy were included in this study. According to the histopathological analysis, 309 (22.27%) nodules were classified as benign, and the rest (n=890, 77.73%) were classified as malignant. The most common benign nodules were related to inflammatory pseudotumor, chronic inflammation, and tuberculosis. On the other hand, in the malignant group, invasive adenocarcinoma was the most common histological subtype. The baseline characteristics of the benign and malignant groups are summarized in Table I. There were no significant differences in gender, age, smoking history, family history, lung nodule location, boundary, calcification sign, and mediastinal lymph node between the two groups ($p>0.05$). Conversely, the long diameter, short diameter, lobulated sign, burr sign, satellite focus, density, vascular convergence sign, and pleural indentation sign differed significantly between the two groups ($p<0.05$). The difference in drinking history between the two groups was borderline statistically significant ($p=0.057$) and was, therefore, still included in the multivariate logistic regression analysis.

Multivariate Logistic Regression Analysis-Forest Plot Model

The factors that were found to be significant in the univariate logistic regression analysis were included in the multivariate logistic regression. Based on this analysis, pulmonary satellite lesions (HR: 0.13, 95% CI 0.03-0.43) were identified as an independent predictor of benign pulmonary nodules. Conversely, the lobulated sign (HR: 1.46, 95% CI 1.03-2.08), burr sign (HR: 2.11, 95% CI 1.50-2.96), density (partial solidity: HR: 5.72, 95% CI 3.91-8.52; grinding glass: HR: 15.85, 95% CI 9.56-27.29), vascular convergence sign (HR: 2.24, 95% CI 1.55-3.26) and pleural indentation sign (HR: 1.52, 95% CI 1.10-2.21) were identified as independent predictors for malignant pulmonary nodules (Figure 1). The drinking history and lesion diameters were not identified as independent predictors of benign and malignant pulmonary nodules ($p>0.05$).

Decision Tree Model for Predicting Benign and Malignant Pulmonary Nodules

Figure 2 represents the final decision tree model for the recursive partition analysis used to discriminate between benign and malignant pulmonary nodules. The final model consisted of 4 layers and 5 nodes. The analysis identified density as the most important predictor, followed by burr sign, vascular convergence sign, and drinking history. These branch points divided the probability of malignant nodules into three risk groups: high, intermediate, and low, as shown in Table II. Patients with SSNs and ground-glass nodules had an 88.5% probability of malignancy, while those with SNs without the spicule or vascular cluster sign and no drinking history had a malignancy probability of only 30%. The final decision tree model achieved an AUC of 0.746 (95% CI 0.705-0.778), a sensitivity of 0.762, and a specificity of 0.799 (Figure 3).

Discussion

This study evaluated the clinical and CT imaging feature differences between benign and malignant pulmonary nodules. This analysis was then used to establish a decision tree model to distinguish between benign and malignant pulmonary nodules. Our findings identified the nodule density, burr sign, and vascular cluster sign as independent risk factors for malignancy.

Several models have been developed in Western countries to characterize pulmonary nodules, including the Mayo Clinic model[12], the VA model[13], and the Brock University model[14]. However, all these models have several limitations. The Mayo model was developed for the non-Asian North American population[15]. This model achieved an AUC of 0.716[16], which is lower than that obtained in our study and other similar models. The accuracy of this model is limited as not all the patients included in the study had a conclusive pathological result. Those patients with inconclusive results were followed up for 2 years and were classified as benign if they had no significant change within the lesion. Moreover, the model was developed a few years ago and was based on plain X-rays. With the rapid development of medical imaging, the applicability of this model needs to be further improved. 98% of the cases included in the VA model were males, and almost all patients had a smoking history, thus limiting the generalizability of the model. The Brock University model achieved high prediction accuracy with an AUC of 0.94. However, this model was based on a small dataset obtained from the Canadian screening program. Moreover, this model also included variables not typically found in the Chinese population and, therefore, could not be used in our study.

Table I. Baseline characteristics of patients.

Variables	Total (n=1,199)	Benign disease (n=309)	Malignant tumor (n=890)	p
Gender, n (%)				0.421
F	627 (52)	155 (50)	472 (53)	
M	572 (48)	154 (50)	418 (47)	
Age, Median (IQR)	57 (50, 64)	58 (50, 64)	57 (50, 64)	0.597
Smoking history, n (%)				0.64
NO	841 (70)	213 (69)	628 (71)	
YES	358 (30)	96 (31)	262 (29)	
Drinking history, n (%)				0.057
NO	925 (77)	251 (81)	674 (76)	
YES	274 (23)	58 (19)	216 (24)	
Family history, n (%)				0.895
0	1,012 (84)	261 (84)	751 (84)	
1	156 (13)	39 (13)	117 (13)	
2	31 (3)	9 (3)	22 (2)	
Tumor site, n (%)				0.447
Lower left	203 (17)	59 (19)	144 (16)	
Lower right	258 (22)	68 (22)	190 (21)	
Middle right	103 (9)	29 (9)	74 (8)	
Middle left	28 (2)	10 (3)	18 (2)	
Upper left	252 (21)	62 (20)	190 (21)	
Upper right	355 (30)	81 (26)	274 (31)	
Long. diameter, Median (IQR)	1.6 (1.1, 2.2)	1.4 (1, 2)	1.7 (1.2, 2.3)	<0.001
Short diameter, Median (IQR)	1.3 (0.9, 1.7)	1.1 (0.8, 1.5)	1.3 (0.9, 1.8)	<0.001
Lobulated sign, n (%)				0.018
NO	350 (29)	107 (35)	243 (27)	
YES	849 (71)	202 (65)	647 (73)	
Burr sign, n (%)				<0.001
NO	678 (57)	208 (67)	470 (53)	
YES	521 (43)	101 (33)	420 (47)	
Boundary, n (%)				0.855
NO	98 (8)	24 (8)	74 (8)	
YES	1,101 (92)	285 (92)	816 (92)	
Satellite Focus, n (%)				<0.001
NO	1,183 (99)	296 (96)	887 (100)	
YES	16 (1)	13 (4)	3 (0)	
Density, n (%)				<0.001
0	610 (51)	241 (78)	369 (41)	
1	366 (31)	44 (14)	322 (36)	
2	223 (19)	24 (8)	199 (22)	
Calcification sign, n (%)				0.866
NO	1,015 (85)	263 (85)	752 (84)	
YES	184 (15)	46 (15)	138 (16)	
Vascular convergence sign, n (%)				<0.001
NO	792 (66)	251 (81)	541 (61)	
YES	407 (34)	58 (19)	349 (39)	
Pleural indentation sign, n (%)				<0.001
NO	524 (44)	180 (58)	344 (39)	
YES	675 (56)	129 (42)	546 (61)	
Mediastinal lymph node, n (%)				0.125
NO	1,094 (91)	289 (94)	805 (90)	
YES	105 (9)	20 (6)	85 (10)	

Variable		N	Odds ratio		p
Drinking_history	NO	925		Reference	
	YES	274		1.62 (1.13, 2.37)	0.010
Long.diameter.		1199		1.22 (0.78, 1.92)	0.388
Short_diameter		1199		1.53 (0.86, 2.70)	0.148
Lobulated_sign	NO	350		Reference	
	YES	849		1.46 (1.03, 2.08)	0.035
Burr_sign	NO	678		Reference	
	YES	521		2.11 (1.50, 2.96)	<0.001
Satellite_Focus	NO	1183		Reference	
	YES	16		0.13 (0.03, 0.43)	0.002
Density	0	610		Reference	
	1	366		5.72 (3.91, 8.52)	<0.001
	2	223		15.85 (9.56, 27.29)	<0.001
Vascular_convergence.sign	NO	792		Reference	
	YES	407		2.24 (1.55, 3.26)	<0.001
Pleural_indentation.sign	NO	524		Reference	
	YES	675		1.52 (1.10, 2.11)	0.012

0.05 0.10.2 0.5 1 2 5 10 20

Figure 1. Results of multivariate logistic regression analysis.

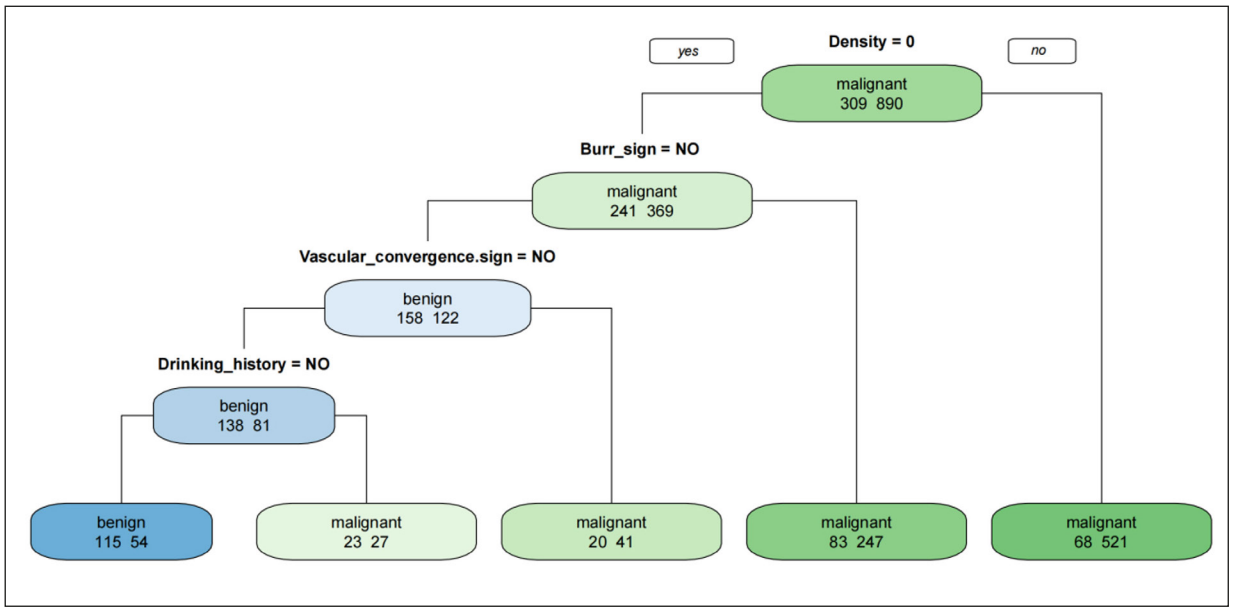

Figure 2. Decision tree model for predicting lung nodule properties.

Table II. Classification of the pulmonary nodules into high, medium, and low risk according to the decision tree model.

Risk groups	Variables
High (70%-100%)	
	Subsolid nodules, ground glass nodules
	Completely solid nodule, burr sign
Moderate (50%-69%)	
	Completely solid nodule, no burr sign, vascular bundle sign
	Completely solid nodule, no burr sign, no vascular bundle sign, drinking history
Low (<50%)	
	Completely solid nodule, no burr sign, no vascular bundle sign, drinking history

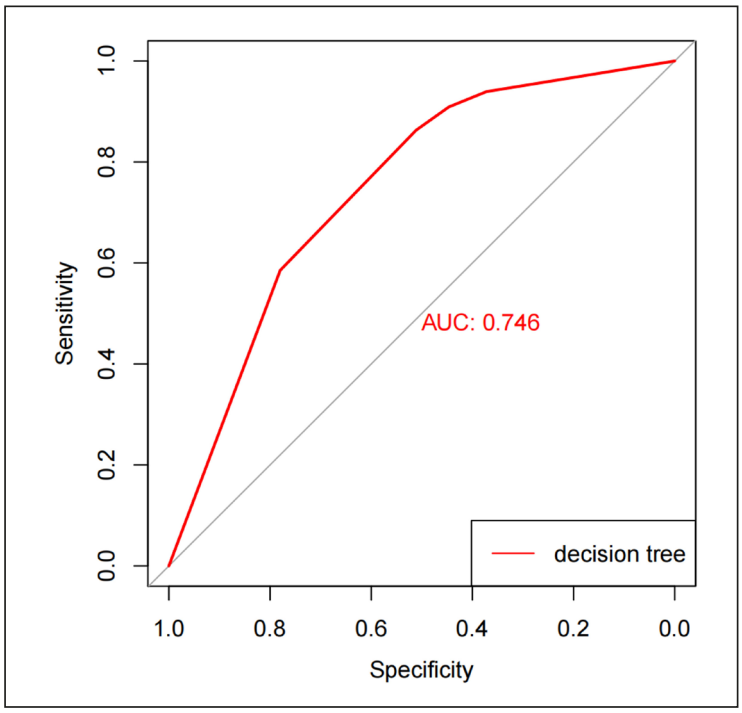

Figure 3. ROC of the training decision tree model. The model achieved an AUC of 0.746, which indicates good prediction accuracy.

The model developed by Li et al[17] is the only model based on Chinese patients. However, when compared with our decision tree model, the Li et al[17] model had a poor prediction accuracy with an AUC of 0.698.

Consistent with previous studies[16,17], our decision tree model identified nodule density as the most important predictor for malignancy. Zhang et al[18] conducted a retrospective analysis of 2,016 nodules and found that the majority (75%) of the SSNs were malignant, while only 39% of the SNs were malignant. Gould et al[19] found that the malignant probability of SSN was 5 times higher than that of SN. Among the subsolid nodules, mixed ground glass nodule (mGGN) had a 63% probability of malignancy and higher than pure ground-glass nodule (pGGN). Multiple guidelines[20,21] recommend using different criteria to distinguish between SN and SNN in clinical practice. Transient SSNs are considered inflammatory lesions, whereas persistent SSNs are deemed to be either preinvasive (atypical adenomatous hyperplasia, adenocarcinoma in situ) or malignant.

In our study, the burr sign was found in 90% of malignant nodules. Pathologically, the development of the spiky sign is associated with increased interlobular interstitial thickness, fibrosis due to occlusion of small peripheral vessels, or cancerous lymphatic vessels[22]. Classical predictive models such as the Mayo Clinic model, the Brock University_model, and the Li et al[17] model also identified the burr sign as one of the risk factors for malignant pulmonary nodules.

The vascular cluster sign was first reported in 1990 by Mori et al[23]. This pattern occurs when multiple small blood vessels converge toward a central point. Noguchi et al[24] reported that a fibrotic reaction is the main mechanism leading to the abnormal formation of peripheral small blood vessels in malignant GGN. Gao et al[25] found that lesions with a regular distribution of blood vessels tend to be benign. On the other hand, lesions with an abnormal distribution of the blood vessels and irregularly shaped boundaries tend to be malignant. In this study, the malignant group had a significantly higher vascular cluster sign rate than the benign group.

Limitations

Our prediction model has some limitations that have to be acknowledged. The data used to construct our model were obtained from a single center, thus limiting the generalizability of the model. The model was based on 2-dimensional (2D) CT data rather than 3-dimensional CT data. In addition, some important clinical factors, such as tumor markers, could not be retrieved from the patient's medical record. The addition of 3D-CT data and other clinical features could improve the prediction performance of the model.

Conclusions

In this study, we developed a decision tree model to characterize pulmonary nodules on CT. The nodule density, burr sign, and vascular cluster sign were identified as the main clinical risk factors for malignancy and were used to develop the final decision tree model. Overall, our model achieved a higher prediction accuracy than other models established in the literature. Therefore our model provides a simple, cost-effective method to characterize CT pulmonary nodules clinically.

Acknowledgments
We appreciate the linguistic assistance provided by TopEdit (www.topeditsci.com) during the preparation of this manuscript.

Availability Data and Materials
The data used to support the findings of this study are available from the corresponding author upon request.

Conflict of Interests
The authors declare that they have no competing interests.

Ethics Approval
The study was conducted according to the guidelines of the Declaration of Helsinki, and approved by the Ethics Committee of the Provincial Hospital Affiliated to Shandong First Medical University (acceptance number: SWYX:NO. 2021-054).

Informed Consent
The IRB approved the application for exemption from informed consent.

Authors' Contributions
Xiaobin Ma and Quanlin Xu contributed equally to this article. Xiaobin Ma, Huaichen Li and Shujuan Jiang performed the conception and design of study; Xiaobin Ma and Quanlin Xu did the statistical analyses and wrote the manuscript; Ning Li and Lina Wang extracted and inputted the data. All authors have read and agreed to the published version of the manuscript.

Funding
This work was funded by the the Natural Science Foundation of Shandong Province, China (No. ZR2021QH334); Shandong Provincial Hospital Scientific Research Incubation Fund (No. 2020FY023); Shandong First Medical University High-level Thesis Cultivation Fund.

ORCID ID
Xiaobin Ma: 0000-0002-4089-8471
Quanlin Xu: 000-0001-9598-1195
Ning Li: 0000-0002-3437-5404
Lina Wang: 0000-0002-9679-5666
Huaichen Li: 0000-0003-2920-8684
Shujuan Jiang: 0000-0003-4197-5966

References

1) Ferlay J, Soerjomataram I, Dikshit R, Eser S, Mathers C, Rebelo M, Parkin DM, Forman D, Bray F. Cancer incidence and mortality worldwide: sources, methods and major patterns in GLOBOCAN 2012. Int J Cancer 2015; 136: E359-E386.
2) Siegel RL, Miller KD, Jemal A. Cancer statistics, 2018. CA Cancer J Clin 2018; 68: 7-30.
3) Smith RA, Andrews KS, Brooks D, Fedewa SA, Manassaram-Baptiste D, Saslow D, Brawley OW, Wender RC. Cancer screening in the United States,2017: A review of current American Cancer Society guidelines and current issues in cancer screening. CA Cancer J Clin 2017; 67: 100-121.
4) National Lung Screening Trial Research Team, Church TR, Black WC, Aberle DR, Berg CD, Clingan KL, Duan F, Fagerstrom RM, Gareen IF, Gierada DS, Jones GC, Mahon I, Marcus PM, Sicks JD, Jain A, Baum S. Results of initial low-dose computed tomographic screening for lung cancer. N Engl J Med 2013; 368: 1980-1991.
5) Liu SQ, Ma XB, Song WM, Li YF, Li N, Wang LN, Liu JY, Tao NN, Li SJ, Xu TT, Zhang QY, An QQ, Liang B, Li HC. Using a risk model for probability of cancer in pulmonary nodules. Thorac Cancer 2021; 12: 1881-1889.
6) Krebs ED, Mehaffey JH, Sarosiek BM, Blank RS, Lau CL, Martin LW. Is less really more? Reexamining video-assisted thoracoscopic versus open lobectomy in the setting of an enhanced recovery protocol. J Thorac Cardiovasc Surg 2020;159: 284-294.e1.
7) Shaukat F, Raja G, Gooya A, Frangi AF. Fully automatic detection of lung nodules in CT images using a hybrid feature set. Med Phys 2017; 44: 3615-3629.
8) Cui X, Heuvelmans MA, Han D, Zhao Y, Fan S, Zheng S, Sidorenkov G, Groen HJM, Dorrius MD, Oudkerk M, de Bock GH, Vliegenthart R, Ye Z. Comparison of veterans affairs, mayo, brock classification models and radiologist diagnosis for classifying the malignancy of pulmonary nodules in chinese clinical population. Transl Lung Cancer Res 2019; 8: 605-613.
9) Truong MT, Ko JP, Rossi SE, Rossi I, Viswanathan C, Bruzzi JF, Marom EM, Erasmus JJ. Update in the evaluation of the solitary pulmonary nodule. Radiographics 2014; 34: 1658-1679.

10) Hansell DM, Bankier AA, MacMahon H, McLoud TC, Müller NL, Remy J. Fleischner Society: Glossary of terms for thoracic imaging. Radiology 2008; 246: 697-722.

11) Biggs D, De Ville B, Suen E. A method of choosing multiway partitions for classification and decision trees. J Appl Stat 1991; 18: 49-62.

12) Swensen SJ, Silverstein MD, Ilstrup DM, Schleck CD, Edell ES. The probability of malignancy in solitary pulmonary nodules. Application to small radiologically indeterminate nodules. Arch Intern Med 1997; 157: 849-855.

13) Gould MK, Ananth L, Barnett PG; Veterans Affairs SNAP Cooperative Study Group. A clinical model to estimate the pretest probability of lung cancer in patients with solitary pulmonary nodules. Chest 2007; 131: 383-388.

14) McWilliams A, Tammemagi MC, Mayo JR, Roberts H, Liu G, Soghrati K, Yasufuku K, Martel S, Laberge F, Gingras M, Atkar-Khattra S, Berg CD, Evans K, Finley R, Yee J, English J, Nasute P, Goffin J, Puksa S, Stewart L, Tsai S, Johnston MR, Manos D, Nicholas G, Goss GD, Seely JM, Amjadi K, Tremblay A, Burrowes P, MacEachern P, Bhatia R, Tsao MS, Lam S. Probability of cancer in pulmonary nodules detected on first screening CT. N Engl J Med 2013; 369: 910-919.

15) Swensen SJ, Silverstein MD, Edell ES, Trastek VF, Aughenbaugh GL, Ilstrup DM, Schleck CD. Solitary pulmonary nodules: clinical prediction model versus physicians. Mayo Clin Proc 1999; 74: 319-329.

16) Zhang M, Zhuo N, Guo Z, Zhang X, Liang W, Zhao S, He J. Establishment of a mathematic model for predicting malignancy in solitary pulmonary nodules. J Thorac Dis 2015; 7: 1833-1841.

17) Li Y, Chen KZ, Sui XZ, Bu L, Zhou ZL, Yang F, Liu YG, Zhao H, Li JF, Liu J, Jiang GH, Wang J. Establishment of a mathematical prediction model for the judgment of benign and malignant solitary pulmonary nodules. Beijing Da Xue Xue Bao Yi Xue Ban 2011; 43: 450-454.

18) Zhang R, Tian P, Chen B, Zhou Y, Li W. Predicting Lung Cancer Risk of Incidental Solid and Subsolid Pulmonary Nodules in Different Sizes. Cancer Manag Res 2020; 12: 8057-8066.

19) Gould MK, Donington J, Lynch WR, Mazzone PJ, Midthun DE, Naidich DP, Wiener RS. Evaluation of individuals with pulmonary nodules: when is it lung cancer? Diagnosis and management of lung cancer, 3rd ed: American College of Chest Physicians evidence-based clinical practice guidelines. Chest 2013; 143: e93S-e120S.

20) Bai C, Choi CM, Chu CM, Anantham D, Chung-Man Ho J, Khan AZ, Lee JM, Li SY, Saenghirunvattana S, Yim A. Evaluation of Pulmonary Nodules: Clinical Practice Consensus Guidelines for Asia. Chest 2016; 150: 877-893.

21) MacMahon H, Naidich DP, Goo JM, Lee KS, Leung ANC, Mayo JR, Mehta AC, Ohno Y, Powell CA, Prokop M, Rubin GD, Schaefer-Prokop CM, Travis WD, Van Schil PE, Bankier AA. Guidelines for Management of Incidental Pulmonary Nodules Detected on CT Images: From the Fleischner Society 2017. Radiology 2017; 284: 228-243.

22) Feng B, Chen X, Chen Y, Liu K, Li K, Liu X, Yao N, Li Z, Li R, Zhang C, Ji J, Long W. Radiomics nomogram for preoperative differentiation of lung tuberculoma from adenocarcinoma in solitary pulmonary solid nodule. Eur J Radiol 2020; 128: 109022.

23) Mori K, Saitou Y, Tominaga K, Yokoi K, Miyazawa N, Okuyama A, Sasagawa M. Small nodular lesions in the lung periphery: new approach to diagnosis with CT. Radiology 1990; 177: 843-849.

24) Noguchi M, Morikawa A, Kawasaki M, Matsuno Y, Yamada T, Hirohashi S, Kondo H, Shimosato Y. Small adenocarcinoma of the lung. Histologic characteristics and prognosis. Cancer 1995; 75: 2844-2852.

25) Gao F, Li M, Ge X, Zheng X, Ren Q, Chen Y, Lv F, Hua Y. Multi-detector spiral CT study of the relationships between pulmonary ground-glass nodules and blood vessels. Eur Radiol 2013; 23: 3271-3277.